PERGAMON

International Journal of Multiphase Flow 27 (2001) 1627–1653

International Journal of Multiphase Flow

www.elsevier.com/locate/ijmulflow

Flow of spatially non-uniform suspensions. Part III: Closure relations for porous media and spinning particles

W. Wang, A. Prosperetti *,[1]

Department of Mechanical Engineering, The Johns Hopkins University, Baltimore, MD 21218, USA

Received 31 July 2000; received in revised form 13 February 2001

Abstract

The methods developed in the earlier papers of this series are applied to the systematic derivation of averaged equations for two situations: slow viscous flow past a system of rigid spheres fixed in space (which may be considered as approximating a porous medium), and the flow induced by a system of fixed spheres all spinning with the same angular velocity. When the same closure relations used in the earlier papers are applied, it is found that the closure coefficients are different. This finding implies that broadly applicable closure relations expressed solely in terms of volume fraction, velocities, and pressure (as usually found in models of the 'two-fluid' type) are insufficient: it must be that one or more additional variables need to be specified to achieve some degree of universality independent of the particular flow considered. It is also shown that the difficulties in the prescription of the viscosity parameter for use in the Brinkman equation derive from the fact that the correct parameter is actually the combination of two different viscosities that accidentally end up combined into a single term when the particles are fixed.

1. Introduction

In parts I and II of this study (Marchioro et al., 2000, 2001), we have described a method for the systematic derivation of closure relations for the averaged equations describing the slow viscous flow of a fluid containing equal suspended rigid spheres. The Introductions of those papers give a description of the background and motivations for this work. In this paper, we apply the same methods to two other flow situations. In the first one the particles do not rotate and translate with the same velocity which, without loss of generality, is taken to vanish: the situation can therefore

* Corresponding author.

[1] Also at: Faculty of Applied Physics and Twente Institute of Mechanics, University of Twente, AE 7500 Enschede, Netherlands, and Burgerscentrum, Netherlands.

0301-9322/01/$ - see front matter
PII: S0301-9322(01)00018-0

be interpreted as modeling pressure-driven flow through a porous medium. The second flow is generated by imposing a fixed angular velocity on the spheres keeping their centers fixed. We are thus able to examine whether the same closure relations derived in the earlier papers are also applicable to the ones considered here. Such a degree of 'universality' is of course the implicit postulate lying at the root of attempts at an averaged description of multiphase flow.

Our answer is negative: it does not seem that models solely phrased in terms of volume fractions, mean velocities, and pressure – as usually encountered in 'two-fluid' formulations – possess a closure capable of reproducing all the flow situations examined in the present series of papers. Some comments on the origin of the problem and a possible solution are offered in the final section.

Another interesting point arising from this study is an explanation of the well-known fact that the correct viscosity to use in the Brinkman equation differs from both the viscosity of the pure fluid and the effective viscosity of the mixture (see e.g., Martys et al., 1994). It is shown that two inherently different terms in the stress of the system coalesce into one when the particle velocities are all equal; the Brinkman viscosity therefore, is the combination of the two closure coefficients that arise in these two terms.

The methods and approach of this study are explained in detail in parts I and II and will not be repeated for brevity. Only the essential differences with the earlier work will be pointed out. We refer to the equations in parts I and II by the prefixes I and II before the equation numbers.

2. The averaged equations and their closure

The form of the averaged equations that we use in this paper has been discussed and justified in Marchioro et al. (1999); throughout this paper indices C and D denote the continuous and disperse phases.

We assume that both the fluid and the particles are incompressible so that the mean volumetric flux $\mathbf{u}_\mathrm{m}$ is divergenceless:

$$\boldsymbol{\nabla}\cdot\mathbf{u}_\mathrm{m}=0. \tag{2.1}$$

The relation between $\mathbf{u}_\mathrm{m}$ and the phase-average velocities of the continuous and disperse phases, $\langle\mathbf{u}_{\mathrm{C,D}}\rangle$, is:

$$\mathbf{u}_\mathrm{m}=\beta_\mathrm{C}\langle\mathbf{u}_\mathrm{C}\rangle+\beta_\mathrm{D}\langle\mathbf{u}_\mathrm{D}\rangle, \tag{2.2}$$

where $\beta_{C,D}$ are the volume fractions satisfying $\beta_\mathrm{C}+\beta_\mathrm{D}=1$.

The momentum equation for the continuous phase is given in Eq. (126) of Marchioro et al. (1999) and, with the neglect of inertia and body forces (and after correcting some obvious misprints), is

$$\beta_\mathrm{C}\boldsymbol{\nabla}\cdot(-p_\mathrm{m}\mathbf{I}+\boldsymbol{\Sigma}_\mathrm{C})=-\beta_\mathrm{D}\mathbf{f}-\frac{a^2}{10}[(\boldsymbol{\nabla}n)\times(\boldsymbol{\nabla}\times\mathscr{A})+n\boldsymbol{\nabla}(\boldsymbol{\nabla}\cdot\mathscr{A})]. \tag{2.3}$$

Here p_m is the mixture pressure and $\boldsymbol{\Sigma}_\mathrm{C}$ the mixture stress; both quantities have been analyzed at length in Marchioro et al. (1999). The quantity $\mathscr{A}$ is the mean hydrodynamic force acting on the particles given by

$$\mathscr{A}(\mathbf{x}) = \overline{\int_{|\mathbf{r}|=a} \mathrm{d}S\mathbf{n}\cdot\boldsymbol{\sigma}_{\mathrm{C}}(\mathbf{x}+\mathbf{r})}, \tag{2.4}$$

where the overline denotes the average over the particles instantaneously centered at $\mathbf{x}$, [2] and $\mathbf{n}$ is the unit normal directed out of the particle; since time is immaterial in the situations considered in this paper, we omit its explicit indication. The mean interphase force $\mathbf{f}$ is introduced by decomposing $\mathscr{A}$ as

$$\overline{\int_{|\mathbf{r}|=a} \mathrm{d}S\mathbf{n}\cdot\boldsymbol{\sigma}_{\mathrm{C}}} = v\boldsymbol{\nabla}\cdot(-p_{\mathrm{m}}\mathbf{I}+\boldsymbol{\Sigma}_{\mathrm{C}}) - v\mathbf{f}, \tag{2.5}$$

where $v = (4/3)\pi a^3$ is the volume of the particles, all with the same radius a. The first term in the right-hand side accounts for the part of the force arising due to the large-scale structure of the flow (e.g., the so-called pseudo-buoyancy), while the second term can be identified with the component of the force due to the local flow structure around the particles and will contain contributions due to drag, the Faxèn term, and others.

With this decomposition, the momentum balance for the particles in the unit volume is

$$nv\boldsymbol{\nabla}\cdot(-p_{\mathrm{m}}\mathbf{I}+\boldsymbol{\Sigma}_{\mathrm{C}}) - nv\mathbf{f} + n\overline{\mathbf{b}} = \mathbf{0}, \tag{2.6}$$

where n is the particle number density and $\mathbf{b}$ the non-hydrodynamic force exerted on the particles by external agents such as, in the situations to be considered below, the constraints that keep their position fixed. For future reference we note that, upon eliminating the divergence term between (2.3) and (2.4), and using the fact that the external force must balance the total hydrodynamic force, we find

$$\mathbf{f} = -\frac{\beta_{\mathrm{C}}}{v}\mathscr{A} - \frac{a^2}{10}[(\nabla\mathbf{n})\times(\nabla\times\mathscr{A}) + n\nabla(\nabla\cdot\mathscr{A})]. \tag{2.7}$$

Under the same assumptions, the balance of angular momentum for the particles is

$$\mathbf{M} \equiv a\overline{\int_{|\mathbf{r}|=a} \mathrm{d}S\mathbf{n}\times(\boldsymbol{\sigma}_{\mathrm{C}}\cdot\mathbf{n})} = -\overline{\mathbf{T}}, \tag{2.8}$$

where $\overline{\mathbf{T}}$ is the mean non-hydrodynamic couple acting on the particles.

The closure of the momentum equations was studied in part II, where the mixture stress was expressed as the sum of an isotropic, a symmetric, and an antisymmetric component:

$$(\boldsymbol{\Sigma}_{\mathrm{C}})_{ij} = -q_{\mathrm{m}}\delta_{ij} + \mathsf{S}_{ij} + \varepsilon_{ijl}(\mathsf{R}_l - \varepsilon_{lqr}\partial_q \mathsf{V}_r). \tag{2.9}$$

Closure relations were deduced for each one of the components. These relations contained the particle-fluid "slip" velocity $\mathbf{u}_{\Delta} = \overline{\mathbf{w}} - \mathbf{u}_{\mathrm{m}}$, where $\overline{\mathbf{w}}$ is the mean center-of-mass velocity of the particles, and the analogous relative angular velocity

$$\boldsymbol{\Omega}_{\Delta} = \overline{\boldsymbol{\Omega}} - \frac{1}{2}\boldsymbol{\nabla}\times\mathbf{u}_{\mathrm{m}}, \tag{2.10}$$

[2] This is the *particle average* introduced in the earlier papers.

where $\overline{\boldsymbol{\Omega}}$ is the mean particle angular velocity. In the situations studied in this paper, $\overline{\mathbf{w}}$ vanishes identically and $\boldsymbol{\Omega}$ is either zero or an imposed value equal for all the particles. Keeping these facts in mind, the closure relations of paper II simplify and become:

$$\frac{1}{\mu_C} q_m = -Q_2 \mathbf{u}_m \cdot \boldsymbol{\nabla}\beta_D, \tag{2.11}$$

$$\mathsf{S} = 2(\mu_{eff} - \mu_{\Delta})\mathbf{E}_m + \mu_{\nabla}\mathbf{E}_{\nabla} + 2\mu_1 a^2 \mathbf{E}_m \nabla^2 \beta_D, \tag{2.12}$$

$$\begin{aligned}\frac{1}{\mu_C}\mathsf{V} = {} & -V_1\mathbf{u}_m + V_2 a^2 \mathbf{E}_m \cdot \boldsymbol{\nabla}\beta_D + \left(V_3 - \frac{1}{2}V_4 - V_9\right) a^2 \nabla^2 \mathbf{u}_m + V_5 a^2 \boldsymbol{\nabla}\beta_D \times \boldsymbol{\Omega}_{\Delta} \\ & - a^2 V_7 (\mathbf{u}_m \cdot \boldsymbol{\nabla})\boldsymbol{\nabla}\beta_D - a^2 V_8 \mathbf{u}_m \nabla^2 \beta_D,\end{aligned} \tag{2.13}$$

$$\begin{aligned}\frac{1}{\mu_C}\mathsf{R} = {} & R_1 \boldsymbol{\Omega}_{\Delta} + R_2 a^2 \boldsymbol{\nabla} \times (\mathbf{E}_m \cdot \boldsymbol{\nabla}\beta_D) + \left(R_3 - \frac{1}{2}R_9\right) a^2 \nabla^2 (\boldsymbol{\nabla} \times \mathbf{u}_m) - R_4 \boldsymbol{\nabla} \times \mathbf{u}_m \\ & - R_5 \boldsymbol{\nabla}\beta_D \times \mathbf{u}_m + R_7 a^2 (\boldsymbol{\Omega}_{\Delta} \cdot \boldsymbol{\nabla})\boldsymbol{\nabla}\beta_D + a^2 R_8 \boldsymbol{\Omega}_{\Delta} \nabla^2 \beta_D,\end{aligned} \tag{2.14}$$

$$\begin{aligned}v\mathbf{f} = 6\pi\mu_C a^3 \beta_C \Bigg[& - a^{-2} F_1 \mathbf{u}_m + F_2 \mathbf{E}_m \cdot \boldsymbol{\nabla}\beta_D + \left(F_3 - \frac{1}{2}F_4 - F_9\right) \nabla^2 \mathbf{u}_m + F_5 \boldsymbol{\nabla}\beta_D \times \boldsymbol{\Omega}_{\Delta} \\ & - F_7 (\mathbf{u}_m \cdot \boldsymbol{\nabla})\boldsymbol{\nabla}\beta_D - F_8 \mathbf{u}_m \nabla^2 \beta_D \Bigg],\end{aligned} \tag{2.15}$$

$$\begin{aligned}\frac{n}{\mu_C}\mathbf{M} = {} & -L_1 \boldsymbol{\Omega}_{\Delta} + L_2 a^2 \boldsymbol{\nabla} \times (\mathbf{E}_m \cdot \boldsymbol{\nabla}\beta_D) + \left(L_3 - \frac{1}{2}L_9\right) a^2 \nabla^2 (\boldsymbol{\nabla} \times \mathbf{u}_m) - L_4 \boldsymbol{\nabla} \times \mathbf{u}_m \\ & - L_5 \boldsymbol{\nabla}\beta_D \times \mathbf{u}_m + L_7 a^2 (\boldsymbol{\Omega}_{\Delta} \cdot \boldsymbol{\nabla})\boldsymbol{\nabla}\beta_D + a^2 L_8 \boldsymbol{\Omega}_{\Delta} \nabla^2 \beta_D.\end{aligned} \tag{2.16}$$

All the symbols with a numerical subscript are coefficients that need to be determined; μ_C is the viscosity coefficient of the pure fluid and μ_{eff} is the effective viscosity well-known from the study of uniform suspensions. The other quantities appearing in these equations are the rate of strain of the field $\mathbf{u}_m$:

$$\mathbf{E}_m = \left[\boldsymbol{\nabla}\mathbf{u}_m + (\boldsymbol{\nabla}\mathbf{u}_m)^T\right] \tag{2.17}$$

and a tensor constructed in terms of the 'slip' velocity $\mathbf{u}_{\Delta}$ (see paper II, Eq. 5.9) which, in this case in which $\overline{\mathbf{w}} = 0$, degenerates to

$$\mathbf{E}_{\nabla} = -(1/2)[\mathbf{u}_m \boldsymbol{\nabla}\beta_D + \boldsymbol{\nabla}\beta_D \mathbf{u}_m] + (1/3)(\mathbf{u}_m \cdot \boldsymbol{\nabla}\beta_D)\mathbf{I}. \tag{2.18}$$

The procedure we apply in this paper is the same as in papers I and II and may be summarized as follows:

1. We choose the mixture pressure p_m, the volumetric flow rate $\mathbf{u}_m$, and the particle volume fraction β_D as the fundamental average quantities of the theory and express them in terms of the agents forcing the two flows studied in the paper, namely, an imposed pressure gradient and an imposed particle angular velocity, in both cases with the particle centers fixed; the relation

between average quantities and forcing agents contains coefficients that will be determined from the numerical simulations.
2. We express in the same way the quantities to be closed, namely, S, q_m, V, etc., all of which can be computed numerically according to unambiguous prescriptions given in the earlier papers; once again, the coefficients necessary for this purpose are determined numerically.
3. By substituting the relations mentioned at point 1 into the right-hand sides of Eqs. (2.11)–(2.16) above, and the relations mentioned at point 2 into the left-hand sides, we obtain a series of equations that determine some of the coefficients carrying a numerical subscript in these equations.

For further details on this approach and further consideration the reader is referred to papers I and II.

3. Preliminaries

Eq. (2.3) is the final form of the momentum equation advocated in Marchioro et al. (1999). However, for the present purposes, just as was done in paper I, it is more helpful to start from the slightly different form

$$\nabla \cdot (-p_m \mathbf{I} + 2\mu_C \mathbf{E}_m + \mathbf{\Sigma}_P) = n\mathscr{A}, \tag{3.1}$$

where

$$\mathbf{\Sigma}_P = (p_m - \beta_C \langle p_C \rangle)\mathbf{I} + \beta_D \mathscr{L}, \tag{3.2}$$

with p_C the continuous-phase pressure; $\mathscr{L}$ is a tensor involving surface integrals of higher moments of the traction on the particle surface (see Eq. 7 in Marchioro et al., 2001 or Eq. I,19). Form (2.3) is found by using decomposition (2.5) of $\mathscr{A}$ and writing

$$\begin{aligned} &\nabla \cdot (-\beta_C \langle p_C \rangle \mathbf{I} + 2\mu_C \mathbf{E}_m + \beta_D \mathscr{L}) - n\mathscr{A} \\ &\quad = \nabla \cdot (-p_m \mathbf{I} + \mathbf{\Sigma}_C) - \frac{\beta_D}{v}\mathscr{A} + \frac{a^2}{10}[(\nabla n) \times (\nabla \times \mathscr{A}) + n\nabla(\nabla \cdot \mathscr{A})]. \end{aligned} \tag{3.3}$$

The justification for this procedure is given in detail in Marchioro et al. (1999) and will not be repeated here.

As in parts I and II, we approximate the spatially unbounded fluid-particle systems of present concern by replicating periodically a unit cubic cell of side L containing N particles. The particles are placed at random and a collection of systems so generated constitutes our ensemble. As described in detail in part I, we construct a slightly non-uniform probability distribution on each one of our ensembles characterized by a sinusoidal spatial variation

$$\epsilon \sin \mathbf{k} \cdot \mathbf{x}, \tag{3.4}$$

where $|\mathbf{k}| = 2\pi/L$ and the direction of $\mathbf{k}$ is taken along one of the sides of the unit cell; the parameter ϵ is assumed to be small and only terms of the first order in ϵ are retained.

Due to this underlying periodic structure, all our ensemble and particle averages can be expanded in a Fourier series which is truncated to the first non-uniform mode. For example, the particle number density is

$$n = n^0 + \epsilon n^s \sin \mathbf{k}\cdot\mathbf{x}, \tag{3.5}$$

where n^0, n^s are constants dependent on the volume fraction and on the cell size. Similarly,

$$\beta_{\mathrm{D}} = \beta_{\mathrm{D}}^0 + \epsilon\beta_{\mathrm{D}}^s \sin \mathbf{k}\cdot\mathbf{x}. \tag{3.6}$$

It is shown in part I that

$$\beta_{\mathrm{D}}^0 = \frac{v}{V}N, \quad \beta_{\mathrm{D}}^s = \left(1 - \frac{a^2k^2}{10}\right)vn^s, \tag{3.7}$$

where $V = L^3$ is the volume of the unit cell. It will prove convenient to use the abbreviations

$$\epsilon_s = \epsilon \sin \mathbf{k}\cdot\mathbf{x}, \qquad \epsilon_c = \epsilon \cos \mathbf{k}\cdot\mathbf{x}. \tag{3.8}$$

The sinusoidal spatial dependence exhibited by (3.5) and (3.6) applies to all the average fields, in general including also a term proportional to $\epsilon\cos\mathbf{k}\cdot\mathbf{x}$ that happens to vanish in the expressions for n and β_{D}; for example

$$\mathscr{A} = \mathscr{A}^0 + \mathscr{A}^s\epsilon_s + \mathscr{A}^c\epsilon_c, \tag{3.9}$$

$$\mathbf{u}_{\mathrm{m}} = \mathbf{U}^0 + \mathbf{U}^s\epsilon_s + \mathbf{U}^c\epsilon_c, \tag{3.10}$$

$$\frac{1}{\mu_{\mathrm{C}}}\boldsymbol{\Sigma}_P = \mathbf{L}^0 + \epsilon_s\mathbf{L}^s + \epsilon_c\mathbf{L}^c, \tag{3.11}$$

and so forth. The Fourier coefficients $n^s, \mathscr{A}^s, \mathscr{A}^c$ etc. appearing in these and similar expressions will be suitably parameterized and calculated numerically as mentioned before and detailed in paper II. Note that since, on the particle scale, the cell side L is large, the spatial variation expressed by these relations is slow when measured on the scale a. Furthermore, as a consequence of the sinusoidal dependence on position of the average fields, every derivative introduces an additional power of $k = 2\pi/L$.

Finally, concerning the last term in (3.3), we note that $(\boldsymbol{\nabla}n)\times(\boldsymbol{\nabla}\times\mathscr{A})$ is of order ϵ^2, and hence negligible at the level of accuracy retained in this study. As for the contribution $\boldsymbol{\nabla}(\boldsymbol{\nabla}\cdot\mathscr{A})$, when the decomposition (2.5) for $\mathscr{A}$ is used, it is seen that it would introduce a term $\nabla^2\boldsymbol{\nabla}p_{\mathrm{m}}$ in the momentum equation, which would alter the mathematical nature of the averaged equations requiring additional boundary conditions about which nothing is known. It appears therefore likely that such a term would constitute a higher order correction and may be expected to be negligible so that $\boldsymbol{\nabla}(\boldsymbol{\nabla}\cdot\mathscr{A}) \simeq -v\boldsymbol{\nabla}(\boldsymbol{\nabla}\cdot\mathbf{f})$.

4. Mean pressure and volumetric flux

As in paper I, rather than calculating p_{m} and the mixture volumetric flow rate $\mathbf{u}_{\mathrm{m}}$ directly from their definition as ensemble averages, it is more convenient to use the averaged momentum equation (3.1) which may be rewritten as

$$-\boldsymbol{\nabla}p_{\mathrm{m}} + \mu_{\mathrm{C}}\nabla^2\mathbf{u}_{\mathrm{m}} + \boldsymbol{\nabla}\cdot\boldsymbol{\Sigma}_{\mathrm{P}} = n\mathscr{A}. \tag{4.1}$$

Upon taking the divergence of this relation and recalling the incompressibility condition (2.1) we find

$$\nabla^2 p_{\mathrm{m}} = \mathbf{\nabla\nabla} : \mathbf{\Sigma}_{\mathrm{P}} - \mathbf{\nabla} \cdot (n\mathscr{A}). \tag{4.2}$$

The divergence of the viscous stress for a spatially uniform system, $\mathbf{\nabla} \cdot \mathbf{L}^0$, must be a constant and, therefore, $\mathbf{\nabla\nabla} : \mathbf{L}^0 = 0$. Upon recalling Eqs. (3.5) and (3.9) and dropping terms of order ϵ^2, we find from (4.2):

$$\nabla^2 p_{\mathrm{m}} = -k^2 \mu_{\mathrm{C}} \mathbf{m} \cdot (\mathbf{L}^s \epsilon_s + \mathbf{L}^c \epsilon_c) \cdot \mathbf{m} - k\mathbf{m} \cdot \left[\epsilon_c (n^0 \mathscr{A}^s + n^s \mathscr{A}^0) - \epsilon_s n^0 \mathscr{A}^c\right], \tag{4.3}$$

where $\mathbf{m} = \mathbf{k}/k$. At this point, it is convenient to present different developments for the two flow situations considered in this paper.

4.1. Porous medium

The first situation we consider – which we refer to as a porous medium – is one in which the particles cannot rotate and all have the same translational velocity which, without loss of generality, is taken to vanish. In this case, the flow is forced by a constant imposed pressure gradient $\mathbf{\nabla} p_\infty$.

In the case of a spatially uniform porous medium often treated in the literature (see e.g., Mo and Sangani, 1994), one introduces the permeability $K = K(\beta_{\mathrm{D}})$ that relates the imposed pressure gradient to the volumetric flow rate $\mathbf{U}^0$. Normalized in such a way that $K \to 1$ for $\beta_{\mathrm{D}} \to 0$, this quantity is defined by

$$\mathbf{U}^0 = -\frac{2a^2}{9\beta_{\mathrm{D}}^0 \mu_{\mathrm{C}}} K \mathbf{\nabla} p_\infty. \tag{4.4}$$

In this uniform case the stress reduces to $\mathbf{L}^0$, which vanishes, and the momentum equation (4.1) simply gives

$$-\mathbf{\nabla} p_\infty = n^0 \mathscr{A}^0 = n^0 a \mu_{\mathrm{C}} A^0 \mathbf{U}^0, \tag{4.5}$$

where, from (4.4),

$$A^0 = \frac{6\pi}{K}. \tag{4.6}$$

Fig. 1 shows a graph of K vs. ak as determined from our simulations for $\beta_{\mathrm{D}} = 15\%$ (triangles), 25% (circles) and 35% (squares); the symbols are the numerical results and the lines least-squares fits of the form $A + B(ak)^2$. The fits are seen to match the data very well so that one can have confidence in the extrapolation to $ak = 0$. These extrapolated values are shown as function of β_{D} in Fig. 2; the solid line is a fit of the form

$$K = (1 - \beta_{\mathrm{D}})^{9.712 - 10.66\beta_{\mathrm{D}}} \tag{4.7}$$

in which the numerical constants have been obtained by a least squares fit; the dashed segments in the figure will be explained below.

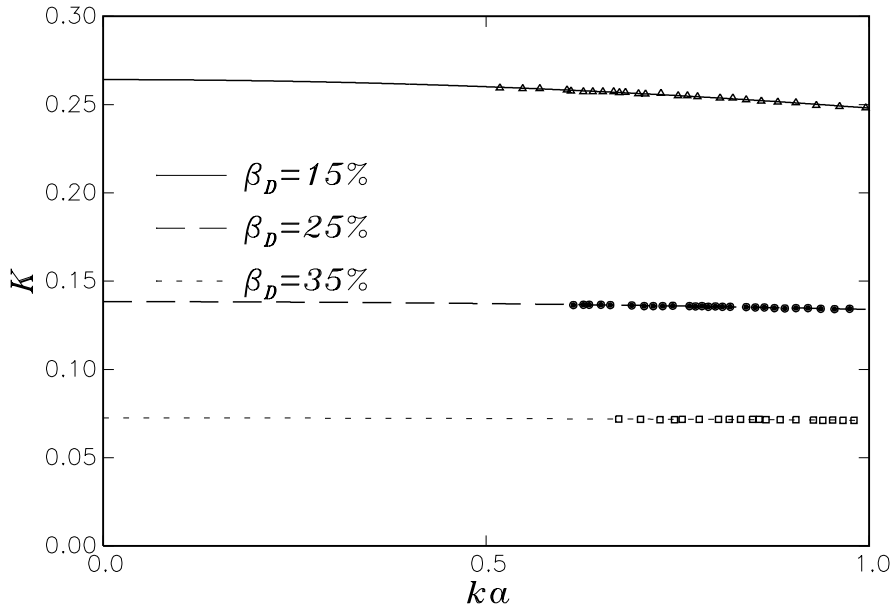

Fig. 1. The dimensionless permeability of a porous medium defined in (4.6) as a function of ka for $\beta_{\mathrm{D}}^{0} = 15\%$ (triangles), 25% (black circles) and 35% (squares); the lines are least-squares fits of the form $A + B(ak)^2$.

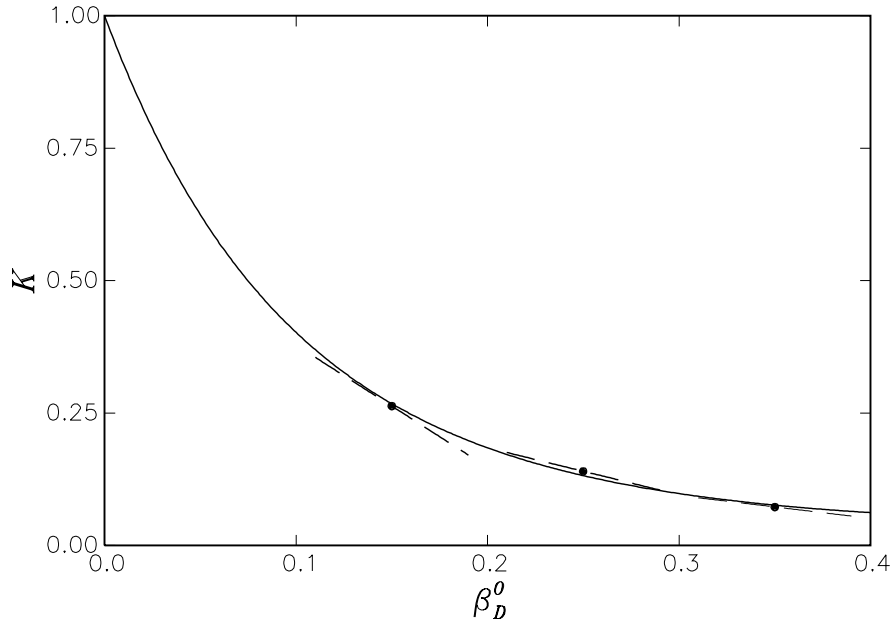

Fig. 2. The dimensionless permeability of a porous medium K evaluated at $ak = 0$ from the previous figure as a function of the disperse-phase volume fraction β_{D}; the points are the computed values and the line the fit (4.7). The dashed segments have the slope given by (5.24).

This same quantity K has also been calculated by Mo and Sangani (1994); for $\beta_D = 25\%$ and 35% we find $K = 0.140$ and 0.0726, to be compared with 0.141 and 0.0704 given in that paper. A discussion of these results is deferred to Section 7.

Let us now turn to the spatially non-uniform situation. Since the flow only occurs due to the imposed pressure gradient and the problem is linear, all vector quantities, such as $\mathscr{A}$, must be linear in ∇p_∞ or, equivalently, in $\mathbf{U}^0$. It proves convenient to introduce the components of $\mathbf{U}^0$ parallel and normal to the particle non-homogeneity by defining

$$\mathbf{U}^0_\parallel = \big(\mathbf{U}^0 \cdot \mathbf{m}\big)\mathbf{m}, \quad \mathbf{U}^0_\perp = (\mathbf{I} - \mathbf{mm}) \cdot \mathbf{U}^0. \tag{4.8}$$

It must then be possible to write

$$\frac{1}{a\mu_C}\mathscr{A} = A^0\mathbf{U}^0 + \sum_{j=s,c} \epsilon_j \Big(A^j_\perp \mathbf{U}^0_\perp + A^j_\parallel \mathbf{U}^0_\parallel \Big). \tag{4.9}$$

By a similar argument, axial vectors and scalars must be proportional to

$$\mathbf{m} \times \mathbf{U}^0, \quad \text{and} \quad \mathbf{U}^0 \cdot \mathbf{m}, \tag{4.10}$$

respectively, since these are the only available quantities with the required tensorial character.

Flow tensors such as $\mathbf{L}$ must be expressible in terms of tensors linear in $\mathbf{U}^0$; as in paper I it proves useful to define

$$\begin{aligned} &\mathbf{G}^U_S = \mathbf{U}^0_\perp \mathbf{m} + \mathbf{m}\mathbf{U}^0_\perp, \quad \mathbf{G}^U_A = \mathbf{U}^0_\perp \mathbf{m} - \mathbf{m}\mathbf{U}^0_\perp, \quad \mathbf{G}^U_I = (\mathbf{U}^0 \cdot \mathbf{m})\mathbf{I}, \\ &\mathbf{G}^U_{\mathrm{m}} = (\mathbf{U}^0 \cdot \mathbf{m})\left(\mathbf{mm} - \frac{1}{3}\mathbf{I} \right), \end{aligned} \tag{4.11}$$

so that, with the superscript $j = s$ or c,

$$k\mathbf{L}^j = \ell^j_S \mathbf{G}^U_S + \ell^j_A \mathbf{G}^U_A + \ell^j_I \mathbf{G}^U_I + \ell^j_M \mathbf{G}^U_M, \tag{4.12}$$

where the factor k in the left-hand side has been introduced to make the coefficients ℓ dimensionless.

The pressure equation (4.3) may be integrated to give, up to an arbitrary constant,

$$\begin{aligned} \frac{1}{\mu_C} p_{\mathrm{m}} = \frac{1}{\mu_C} \mathbf{x} \cdot \nabla p_\infty + \frac{1}{ka^2} \Bigg[&\left(\ell^s_I + \frac{2}{3}\ell^s_M + n^0 a^3 A^c_\perp \right) \epsilon_s \\ &+ \left(\ell^c_I + \frac{2}{3}\ell^c_M - a^3 (n^0 A^s_\parallel + n^s A^0) \right) \epsilon_c \Bigg] (\mathbf{U}^0 \cdot \mathbf{m}). \end{aligned} \tag{4.13}$$

When this expression is substituted into the momentum equation (4.1), the solution for $\mathbf{u}_{\mathrm{m}}$ can be expressed as in (3.10) with

$$\mathbf{U}^s = \frac{1}{k^2 a^2} \big(\ell^c_S + \ell^c_A - n^0 a^3 A^s_\perp \big) \mathbf{U}^0_\perp, \tag{4.14}$$

and a similar result for $\mathbf{U}^c$. The numerical simulations to be described below suggest that $A^c_\perp$, $A^c_\parallel$, ℓ^s_S, and ℓ^s_A all vanish; accepting this fact we conclude that $\mathbf{U}^c = 0$ so that

$$\mathbf{u}_{\mathrm{m}} = \mathbf{U}^0 + U^s \epsilon_s \mathbf{U}^0_\perp, \tag{4.15}$$

where, from (4.14),

$$a^2 k^2 U^s = \ell^c_S + \ell^c_A - n^0 a^3 A^s_\perp. \tag{4.16}$$

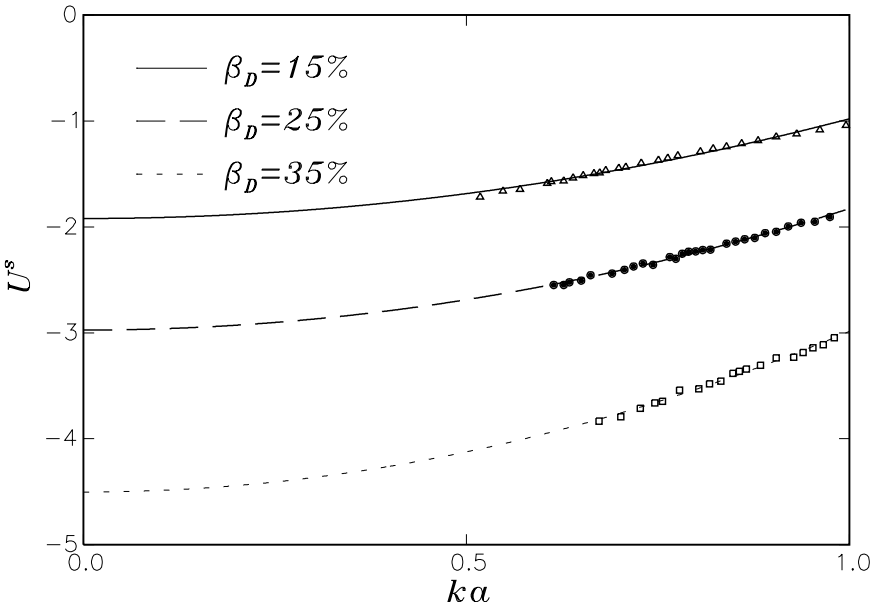

Fig. 3. The quantity U^s appearing in expression (4.16) for the mean fluid velocity in a porous medium as a function of ka for $\beta_{\mathrm{D}}^0 = 15\%$ (triangles), 25% (black circles) and 35% (squares); the lines are least-squares fits of the form $A + B(ak)^2$.

Similarly, the pressure expression (4.13) becomes

$$\frac{1}{\mu_{\mathrm{C}}} p_{\mathrm{m}} = \frac{1}{\mu_{\mathrm{C}}} \mathbf{x} \cdot \boldsymbol{\nabla} p_\infty + \frac{P^c}{ka^2} \epsilon_c (\mathbf{U}_\parallel \cdot \mathbf{m}), \tag{4.17}$$

with

$$P^c = \ell_I^c + \frac{2}{3} \ell_M^c - n^0 a^3 A_\parallel^s - n^s a^3 A^0. \tag{4.18}$$

Fig. 3 shows U^s vs. ak for $\beta_{\mathrm{D}}^0 = 15\%$, 25% and 35%. The scatter of the numerical results is small and the quadratic fits shown by the lines match them well; in particular, note that division by k^2, as implied by (4.16), does seem to bring U^s to a finite value as $ak \to 0$.

In the following, we need expressions for the rate of strain $\mathbf{E}_{\mathrm{m}}$ and for $\mathbf{E}_\nabla$ defined in (2.17) (2.18); with (4.15), these quantities are given by

$$\mathbf{E}_{\mathrm{m}} = \frac{1}{2} U^s \epsilon_c k \mathbf{G}_S^U, \quad \mathbf{E}_\nabla = -\frac{1}{2} k \epsilon_c \beta_{\mathrm{D}}^s \mathbf{G}_S^U - k \epsilon_c \beta_{\mathrm{D}}^s \mathbf{G}_M^U, \tag{4.19}$$

while, from Eq. (4.9),

$$n \nabla (\nabla \cdot \mathbf{f}) = a \mu_{\mathrm{C}} n^0 k^2 A_\parallel^s \epsilon_s \mathbf{U}_\parallel^0. \tag{4.20}$$

4.2. Spinning particles

The second situation that we study is characterized by the fact that the particles rotate all with the same angular velocity $\boldsymbol{\Omega}$ maintaining a fixed position. Clearly, in this situation, there would be no net flow if the particle distribution were spatially uniform and, therefore, $\mathbf{U}^0 = 0$. This fact is

intuitively clear, but may also be deduced from the fact that it is impossible to construct a polar vector such as $\mathbf{U}^0$ using only the axial vector $\boldsymbol{\Omega}$ (see also Brenner, 1984).

In a non-uniform system, however, the vector $\mathbf{m}$ is also available and one can construct the polar vector

$$\boldsymbol{\Omega}_\perp = \mathbf{m} \times \boldsymbol{\Omega} \tag{4.21}$$

in terms of which it is possible to express the velocity. The available two-tensors are

$$\mathbf{G}^\Omega_S = \boldsymbol{\Omega}_\perp \mathbf{m} + \mathbf{m}\boldsymbol{\Omega}_\perp, \qquad \mathbf{G}^\Omega_A = \boldsymbol{\Omega}_\perp \mathbf{m} - \mathbf{m}\boldsymbol{\Omega}_\perp. \tag{4.22}$$

Since there is no homogeneous term, we can write the hydrodynamic force as

$$\frac{1}{a\mu_C}\mathscr{A} = 6\pi(\epsilon_s A^s + \epsilon_c A^c)\boldsymbol{\Omega}_\perp, \tag{4.23}$$

and, since no true scalar can be constructed with the vectors $\boldsymbol{\Omega}_\perp$ and $\mathbf{m}$, we must have $p_m = \text{const.}$ and

$$\mathbf{u}_m = a^2 k U^c \epsilon_c \boldsymbol{\Omega}_\perp, \tag{4.24}$$

with

$$a^3 k^3 U^c = (\ell^s_S + \ell^s_A) - \frac{9}{2}\beta^0_D A^c. \tag{4.25}$$

This relation is similar to the earlier one (4.16) but the numerical results exhibit stronger fluctuations, which make it somewhat more difficult to extract U^c. To deal with this problem, as suggested by the dilute-limit results of Eq. (A.7), we fit the two groups of terms in the right-hand side by expressions of the form $ak(A_1 + B_1(ak)^2)$ and $ak(A_2 + B_2(ak)^2)$. Fig. 4 shows the results of such a fit and, even with some differences due to the scatter, does suggest that $A_1 = A_2$ so that the left-hand side of (4.25) is finite as $ak \to 0$.

From (4.24)

$$\mathbf{E}_m = -\frac{1}{2}a^2 k^2 U^c \epsilon_s \mathbf{G}^\Omega_S, \tag{4.26}$$

while $\mathbf{E}_\nabla = \mathrm{O}(\epsilon^2)$ and $\nabla \cdot \mathbf{f} = 0$.

We can now proceed to calculate the closure parameters by implementing the procedure outlined at the end of Section 2. We consider the porous medium case first.

5. Closure: porous medium

As remarked before, all the closure terms have explicit closed-form expressions in terms of quantities that can be calculated numerically. The results of these numerical calculations are averaged and represented in terms of the fundamental scalars, vectors and tensors introduced in the previous section. The manner in which this is done is explained in detail in Marchioro and Prosperetti (1999) and in papers I and II. In the case of the symmetric part of the stress, this procedure leads to a result of the form

$$\frac{1}{\mu_C}\mathsf{S} = k\epsilon_c\left(s^P_S \mathbf{G}^U_S + s^P_M \mathbf{G}^U_M\right). \tag{5.1}$$

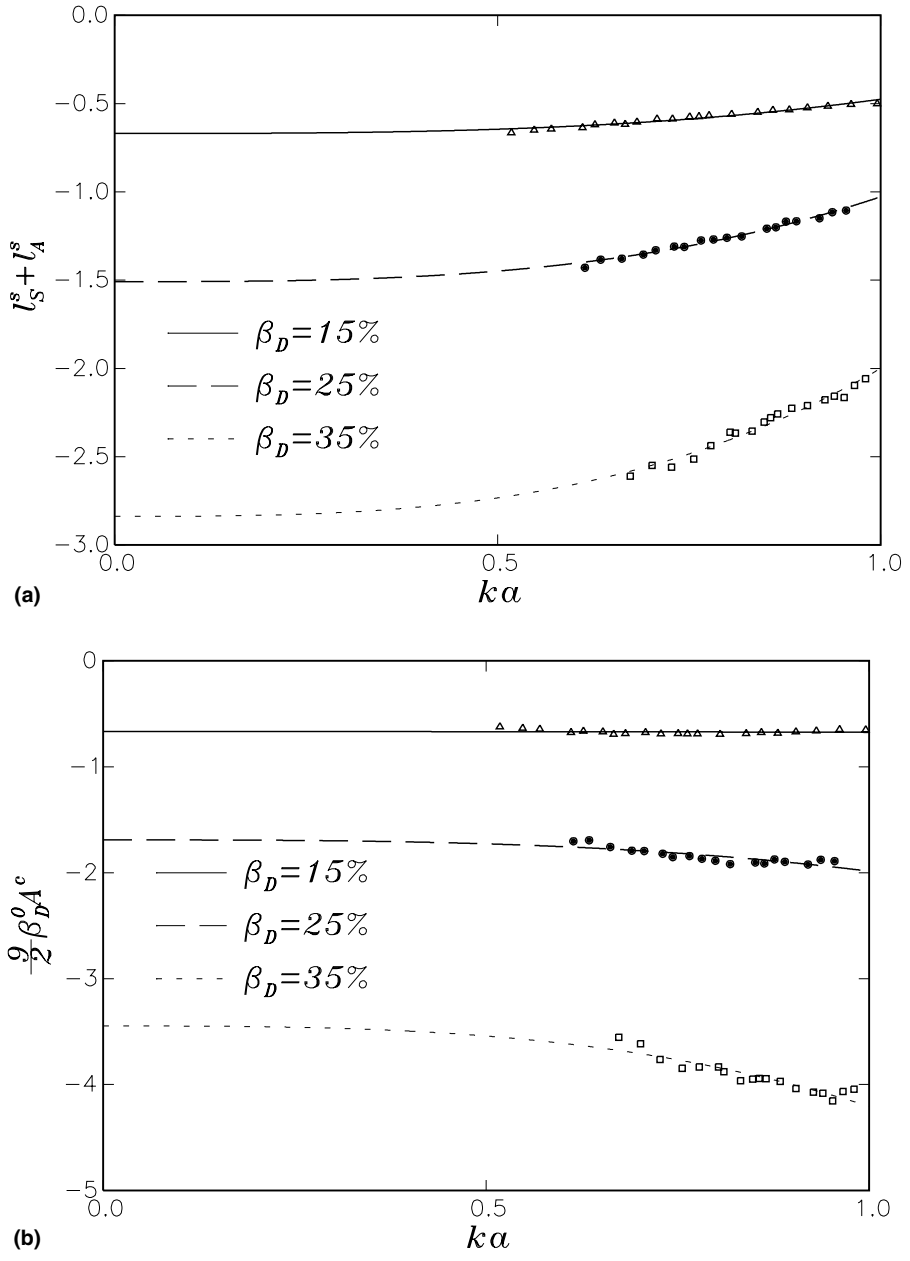

Fig. 4. (a) The quantity $\ell_S^s + \ell_A^s$ appearing in the mean fluid velocity (4.25) for spinning particles as a function of ka for $\beta_{\mathrm{D}}^0 = 15\%$ (triangles), 25% (black circles) and 35% (squares); the lines are least-squares fits of the form $ak(A + B(ak)^2)$ as suggested by (A.7); (b) the quantity $-\frac{9}{2}\beta_{\mathrm{D}}^0 A^c$ plotted similarly.

The coefficients s_S^P and s_M^P as determined from the numerical simulations are shown as functions of ka in Figs. 5 and 6 for $\beta_{\mathrm{D}} = 15\%$, 25% and 35%; as before the lines are quadratic fits of the form $A + B(ak)^2$. The results for $\beta_{\mathrm{D}} = 15\%$ (triangles) and 25% (circles) exhibit an acceptable amount

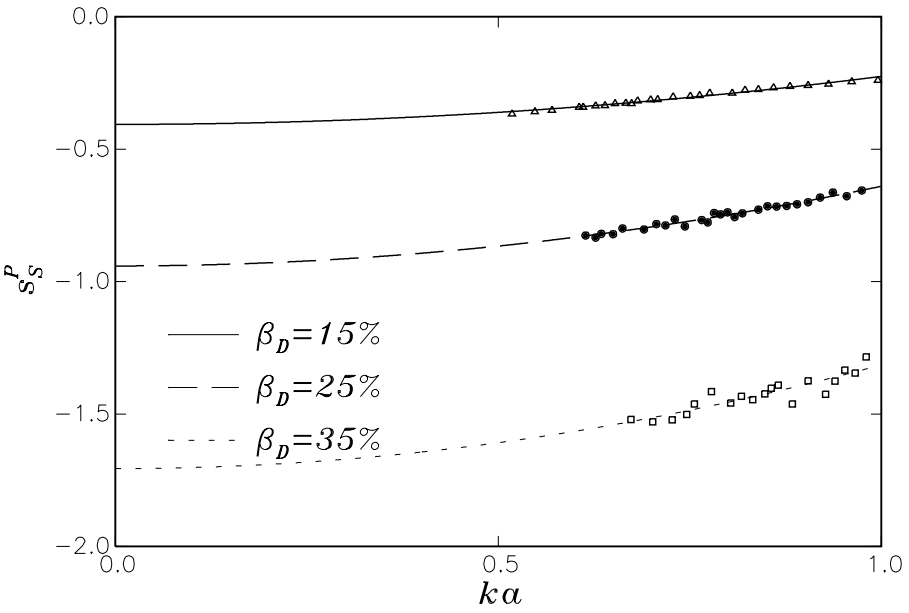

Fig. 5. The quantity s_S^P appearing in expression (5.1) of the stress for a porous medium as a function of ka for $\beta_{\mathrm{D}}^0 =$ 15% (triangles), 25% (black circles) and 35% (squares); the lines are least-squares fits of the form $A + B(ak)^2$.

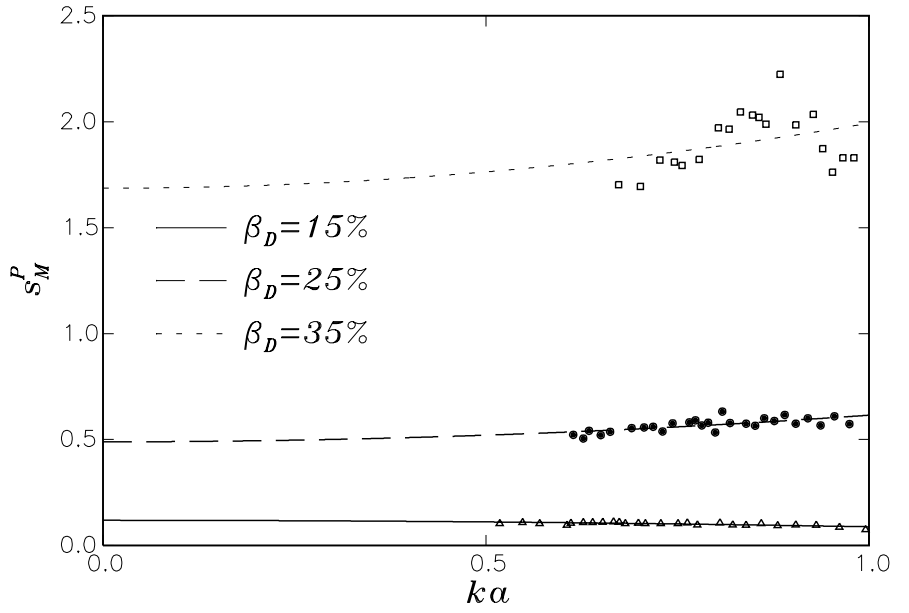

Fig. 6. The quantity s_M^P appearing in the expression for stress (5.1) for a porous medium as a function of ka for $\beta_{\mathrm{D}}^0 =$ 15% (triangles), 25% (black circles) and 35% (squares); the lines are least-squares fits of the form $A + B(ak)^2$.

of scatter, while those for 35% are not smooth; this is probably a consequence of the use of only five singularities to describe the particles, which limits the numerical accuracy at the higher volume fractions.

Upon substituting the expressions (4.19) for $\mathbf{E}_{\mathrm{m}}, \mathbf{E}_{\nabla}$ into (2.12), the symmetric part of the average stress becomes

$$\mathsf{S} = \left[(\mu_{\mathrm{eff}} - \mu_{\Delta})U^s - \mu_{\nabla}\beta^s_{\mathrm{D}}\right]k\epsilon_c\mathbf{G}^U_S + \mu_{\nabla}\beta^s_{\mathrm{D}}k\epsilon_s\mathbf{G}^U_M. \tag{5.2}$$

Upon comparing (5.1) and (5.2), we thus have

$$\frac{\mu_{\mathrm{eff}} - \mu_{\Delta}}{\mu_{\mathrm{C}}}U^s - \beta^s_{\mathrm{D}}\frac{\mu_{\nabla}}{\mu_{\mathrm{C}}} = s^P_S, \tag{5.3}$$

$$\beta^s_{\mathrm{D}}\frac{\mu_{\nabla}}{\mu_{\mathrm{C}}} = s^P_M. \tag{5.4}$$

For the reasons explained in parts I and II, we are interested in the limit of these relations as $ak \to 0$; the values of $\mu_{\mathrm{eff}} - \mu_{\Delta}$ and μ_{∇} obtained in this limit are shown in Table 1; those for μ_{∇} can be fitted by

$$\frac{\mu_{\nabla}}{\mu_{\mathrm{C}}} = 32.7\beta^{2.38}_{\mathrm{D}}. \tag{5.5}$$

Some considerations on these results will be given in Section 7.

According to (4.10), the numerical results for the isotropic part of the stress q_{m} can be parameterized as

$$\frac{1}{\mu_{\mathrm{C}}}q_{\mathrm{m}} = -q^P k\epsilon_c\mathbf{U}^0\cdot\mathbf{m}, \tag{5.6}$$

while, from the closure ansatz (2.11),

$$\frac{1}{\mu_{\mathrm{C}}}q_{\mathrm{m}} = -Q_2\beta^s_{\mathrm{D}}\epsilon_c\mathbf{U}^0\cdot\mathbf{m}, \tag{5.7}$$

from which, upon comparing and taking the limit $(ak) \to 0$, we have

$$Q_2 = \lim_{ka\to 0}\frac{q^P}{\beta^s_{\mathrm{D}}}. \tag{5.8}$$

The calculated values of q^P are shown in Fig. 7 vs. ak. Numerical values for Q_2 obtained from this relation are given in Table 1 and plotted as a function of β_{D} in Fig. 8; the line is a fit of the form

$$Q_2 = 558\beta^{4.55}_{\mathrm{D}}. \tag{5.9}$$

The term corresponding to Q_2, being an isotropic contribution to the stress, may be considered as a pressure effect due to the flow; thus, its rapid rising with increasing volume fraction is not surprising (Tables 1 and 2).

Table 1
Values of the closure parameters for the porous medium simulations at three volume fractions in the limit $ak \to 0$

β_{D} (%)	$(\mu_{\mathrm{eff}} - \mu_{\Delta})/\mu_{\mathrm{C}}$	$\mu_{\nabla}/\mu_{\mathrm{C}}$	K	Q_2	V_1
15	0.150	0.392	0.263	~ 0	0.069
25	0.174	0.989	0.140	1.03	0.186
35	0.0391	3.06	0.0726	4.70	0.414

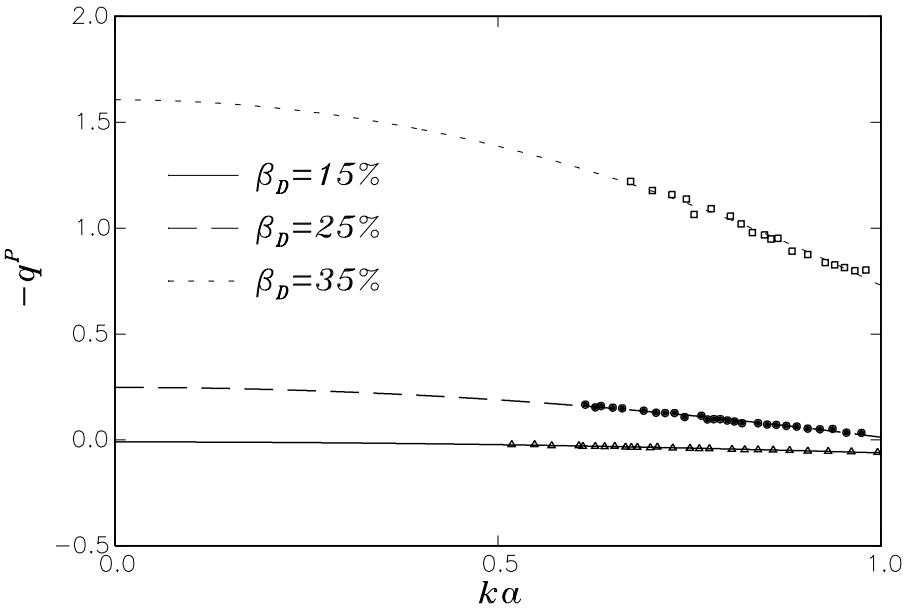

Fig. 7. The quantity q^P appearing in the isotropic part of the stress for a porous medium, Eq. (5.6), as a function of ka for $\beta_{\mathrm{D}}^0 = 15\%$ (triangles), 25% (black circles) and 35% (squares); the lines are least-squares fits of the form $A + B(ak)^2$.

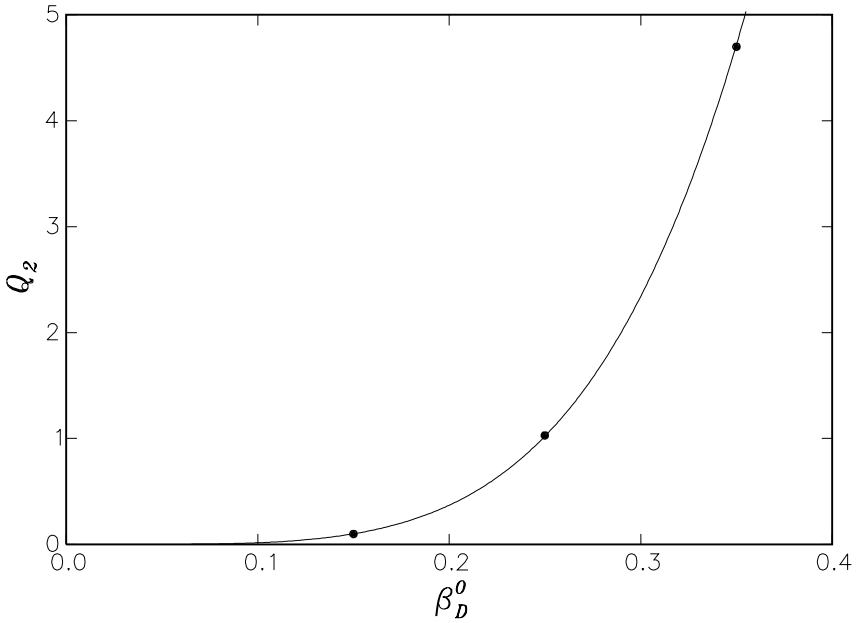

Fig. 8. The values of the coefficient Q_2 of the isotropic part of the stress for a porous medium evaluated from (5.8) as a function of the disperse-phase volume fraction β_{D}; the points are the computed values and the line the fit (5.9).

Table 2
Values of the closure parameters for the spinning particles simulations at three volume fractions

β_D (%)	$(\mu_{eff} - \mu_A)/\mu_C$	F_1	V_1	L_1
15	0.410	4.12	0.0623	1.34
25	0.174	7.51	0.166	1.59
35	0.0391	12.6	0.351	1.89

Omitting the terms proportional to ϵ_c, which are found to vanish, we parameterize the numerical results for the polar vector of the antisymmetric part of the stress similarly to (4.9), i.e.,

$$\frac{1}{\mu_C}\mathbf{V} = v^0\mathbf{U}^0 + (v^P_\parallel \mathbf{U}^0_\parallel + v^P_\perp \mathbf{U}^0_\perp)\epsilon_s, \tag{5.10}$$

while, from the closure relation (2.13), we have

$$\frac{1}{\mu_C}\mathbf{V} = V_1\mathbf{U}^0 + \left[U^s\left(V_1 + k^2a^2\left(V_3 - \frac{1}{2}V_4 - V_9\right)\right) - \left(\frac{1}{2}V_5 - V_8\right)\beta^s_D k^2a^2\right]\epsilon_s\mathbf{U}^0_\perp - \left(\frac{1}{2}V_5 + V_7 - V_8\right)k^2a^2\beta^s_D\epsilon_s\mathbf{U}^0_\parallel. \tag{5.11}$$

Upon comparing, we find the three relations

$$V_1 = \lim_{ak\to 0} v^0, \tag{5.12}$$

$$0 = v^P_\parallel + a^2k^2\left(\frac{1}{2}V_5 + V_7 - V_8\right)\beta^s_D, \tag{5.13}$$

$$\frac{dV_1}{d\beta_D}\beta^s_D + U^s\left[V_1 + k^2a^2\left(V_3 - \frac{1}{2}V_4 - V_9\right)\right] = v^P_\perp + a^2k^2\left(\frac{1}{2}V_5 - V_8\right)\beta^s_D. \tag{5.14}$$

The parameter v^0 is shown as a function of ak in Fig. 9 for three volume fractions; the scatter is minimal and the zero-intercepts, giving V_1, well defined. The corresponding values are given in Table 1 and plotted as a function of β_D in Fig. 10; the line is a fit of the form [3]

$$V_1 = 3.626\beta_D^{2.10}. \tag{5.15}$$

For consistency of (5.13) the limit of $v^P_\parallel$ for $ak \to 0$ should vanish; the numerical results suggest values of the order of 10^{-4} – 10^{-3}, which is compatible with 0 given the present numerical accuracy. In the limit $ak \to 0$, the last relation (5.14) gives

$$\frac{dV_1}{d\beta_D}\beta^s_D + U^sV_1 = v^P_\perp. \tag{5.16}$$

Segments with the slope $dV_1/d\beta_D$ given by this relation are shown by the dotted lines in Fig. 10; the numerical values obtained from the fit (5.15) are 1.142, 1.904, 2.665, respectively, for β_D = 15%, 25% and 35%, while those found from (5.16) are 1.069, 1.719, 2.770.

[3] If the exponent is changed from 2.10 to 2, the prefactor changes from 3.626 to 3.136.

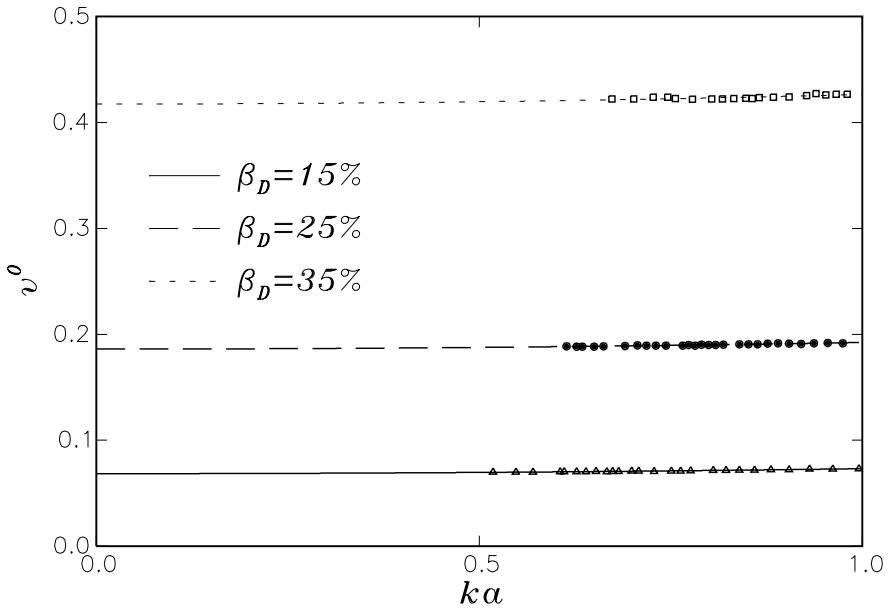

Fig. 9. The quantity v^0 appearing in the polar vector component of the antisymmetric stress of a porous medium, Eq. (5.10), as a function of ka for $\beta_{\mathrm{D}}^0 = 15\%$ (triangles), 25% (black circles) and 35% (squares); the lines are least-squares fits of the form $A + B(ak)^2$.

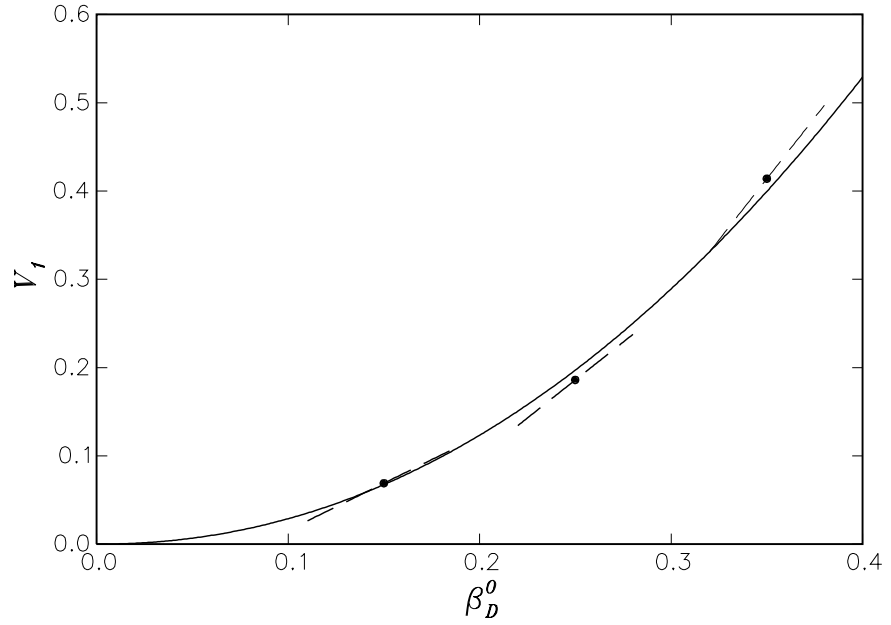

Fig. 10. The coefficient V_1 of the polar vector component of the antisymmetric stress of a porous medium evaluated from the zero-intercept of v^0 shown in the previous figure according to (5.12) as a function of the disperse-phase volume fraction β_{D}; the points are the computed values and the line the fit (5.15). The dashed segments have the slope given by (5.16).

The numerical results for the axial vector $\mathbf{R}$ of the antisymmetric part of the stress can be parameterized as

$$\frac{1}{\mu_C}\mathbf{R} = r^c v\epsilon_c k\mathbf{m}\times\mathbf{U}^0, \tag{5.17}$$

from which, upon comparing with (2.14),

$$r^c = \left[\left(\frac{1}{2}R_1 - R_4\right) + k^2a^2\left(R_3 - \frac{1}{2}R_9\right)\right]U^s - R_5\beta_D^s, \tag{5.18}$$

and, as $(ka)\to 0$,

$$r^c = \left(\frac{1}{2}R_1 - R_4\right)U^s - R_5\beta_D^s. \tag{5.19}$$

Unfortunately the present flow situation does not give sufficient information for the determination of any of the closure parameters for $\mathbf{R}$.

By substituting (4.9), (4.20) and (4.15) into Eq. (2.7), we find that the numerical results for $\mathbf{f}$ can be written as

$$v\mathbf{f} = -a\mu_C\beta_C^0\left[A^0\mathbf{U}^0 + \epsilon_s A_\parallel^s\left(1 - k^2a^2\beta_D^0\right)\mathbf{U}_\parallel^0 + \epsilon_s A_\perp^s\mathbf{U}_\perp\right], \tag{5.20}$$

while, from the closure relation (2.15), we have

$$v\mathbf{f} = 6\pi\mu_C a\beta_C\left[F_1\mathbf{U}^0 + \left(F_1 + a^2k^2\left(F_3 - \frac{1}{2}F_4 - F_9\right)\right)U^s\epsilon_s\mathbf{U}_\perp^0 - a^2k^2F_8\beta_D^s\epsilon_s\mathbf{U}^0\right]. \tag{5.21}$$

Upon comparing,

$$F_1 = \frac{1}{K(\beta_D^0)}, \tag{5.22}$$

$$\frac{dF_1}{d\beta_D}\beta_D^s + \left[F_1 + k^2a^2\left(F_3 - \frac{1}{2}F_4 - F_9\right)\right]U^s = A_\perp^s + a^2k^2\left(\frac{1}{2}F_5 - F_8\right)\beta_D^s. \tag{5.23}$$

Upon eliminating F_1 between these two relations and taking the limit $(ak)\to 0$, we have

$$\frac{dK}{d\beta_D} = \frac{K}{\beta_D^s}(U^s - KA_\perp^s), \tag{5.24}$$

which should be consistent with the expression of K given in (4.7). As before, segments with the slope given by this relation are shown by the dotted lines in Fig. 2; numerically, Eq. (4.7) gives −2.090, −0.8535, −0.3505 for $\beta_D = 15\%$, 25% and 35%, while, from (5.24), we have −2.307, −0.8881, −0.4325, respectively. A good degree of consistency is therefore observed.

Proceeding in the same way in the case of the hydrodynamic couple given by (2.16) we start by writing, as in (4.10),

$$\frac{1}{\mu_C}\mathbf{M} = m^c v\epsilon_c k\mathbf{m}\times\mathbf{U}^0, \tag{5.25}$$

which, upon comparison with (2.16), leads to

$$n^0 m^c = \left[((1/2)L_1 - L_4) + k^2 a^2 (L_3 - (1/2)L_9)\right] U^s - L_5 \beta^s_{\mathrm{D}}, \tag{5.26}$$

from which, as $(ka) \to 0$,

$$n^0 m^c = ((1/2)L_1 - L_4) U^s - L_5 \beta^s_{\mathrm{D}}. \tag{5.27}$$

Here, the situation is similar to that encountered before for $\mathbf{R}$ and none of the coefficients can be determined.

6. Spinning particles closure

The procedure for the case of particles with an imposed angular velocity is identical to that followed in the previous section. The situation is somewhat simpler as the isotropic part of the stress q_{m} is readily seen from (2.11) to vanish, which is consistent with the numerical results; the axial part of the antisymmetric component of the stress also vanishes.

The analog of Eqs. (5.1), (5.10), and (5.20), (5.25) are

$$\mathsf{S} = -(\mu_{\mathrm{eff}} - \mu_{\Delta}) a^2 k^2 U^c \epsilon_s \mathbf{G}^{\Omega}_S, \tag{6.1}$$

$$\frac{1}{\mu_{\mathrm{C}}} \mathbf{V} = \left[V_1 + a^2 k^2 \left(- V_3 + \frac{1}{2} V_4 + V_9 \right) \right] U^c a^2 k \epsilon_c \boldsymbol{\Omega}_{\perp}, \tag{6.2}$$

$$v\mathbf{f} = -6\pi \mu_{\mathrm{C}} a \beta_{\mathrm{C}} \left[F_1 + a^2 k^2 \left(F_3 - \frac{1}{2} F_4 - F_9 \right) \right] a^2 k U^c \epsilon_c \boldsymbol{\Omega}_{\perp}, \tag{6.3}$$

$$\frac{n}{\mu_{\mathrm{C}}} \mathbf{M} = -L_1 \boldsymbol{\Omega} + \left[\frac{1}{2} L_1 - L_4 + k^2 a^2 \left(L_3 - \frac{1}{2} L_9 \right) \right] U^c k^2 a^2 \epsilon_s \mathbf{m} \times \boldsymbol{\Omega}_{\perp}, \tag{6.4}$$

while a direct calculation on the basis of the right-hand sides of (2.12), (2.13), (2.15), and (2.16) gives

$$\frac{1}{\mu_{\mathrm{C}}} \mathsf{S} = -s^{\Omega}_S \epsilon_s a^2 k^2 \mathbf{G}^{\Omega}_S, \tag{6.5}$$

$$\frac{1}{\mu_{\mathrm{C}}} \mathbf{V} = v^c a^2 k \epsilon_c \boldsymbol{\Omega}_{\perp}. \tag{6.6}$$

$$v\mathbf{f} = 6\pi \beta_{\mathrm{C}} \mu_{\mathrm{C}} a^2 \epsilon_c A^c \boldsymbol{\Omega}_{\perp}, \tag{6.7}$$

$$\frac{n}{\mu_{\mathrm{C}}} \mathbf{M} = -m^0 \boldsymbol{\Omega} + m^s \epsilon_s k^2 a^2 \mathbf{m} \times \boldsymbol{\Omega}_{\perp}. \tag{6.8}$$

Figs. 11 and 12 show the calculated values of s^{Ω}_S and v^c as functions of ka and Fig. 13 gives m^0; a graph for A^c was provided in Fig. 4(b).

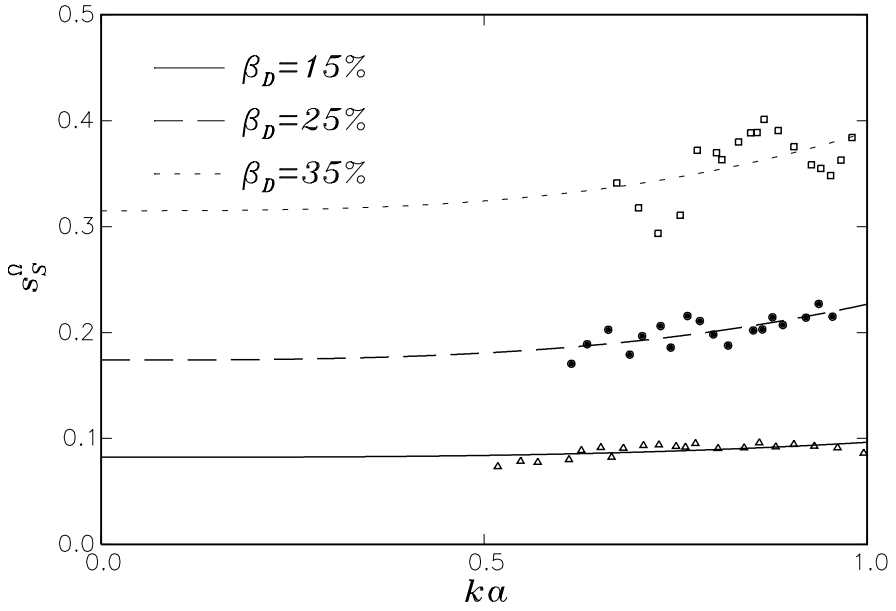

Fig. 11. The quantity s_S^{Ω} appearing in the expression for stress (6.5) for a system with spinning particles as a function of ka for $\beta_{\mathrm{D}}^0 = 15\%$ (triangles), 25% (black circles) and 35% (squares); the lines are least-squares fits of the form $A + B(ak)^2$.

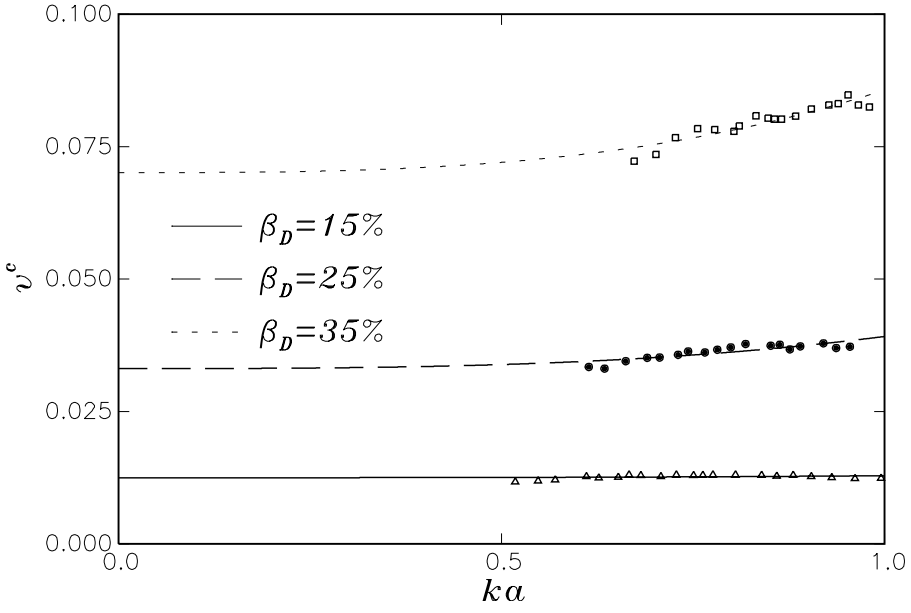

Fig. 12. The quantity v^c appearing in the polar vector component of the antisymmetric stress of a spinning particle system in Eq. (6.6) as a function of ka for $\beta_{\mathrm{D}}^0 = 15\%$ (triangles), 25% (black circles) and 35% (squares); the lines are least-squares fits of the form $A + B(ak)^2$.

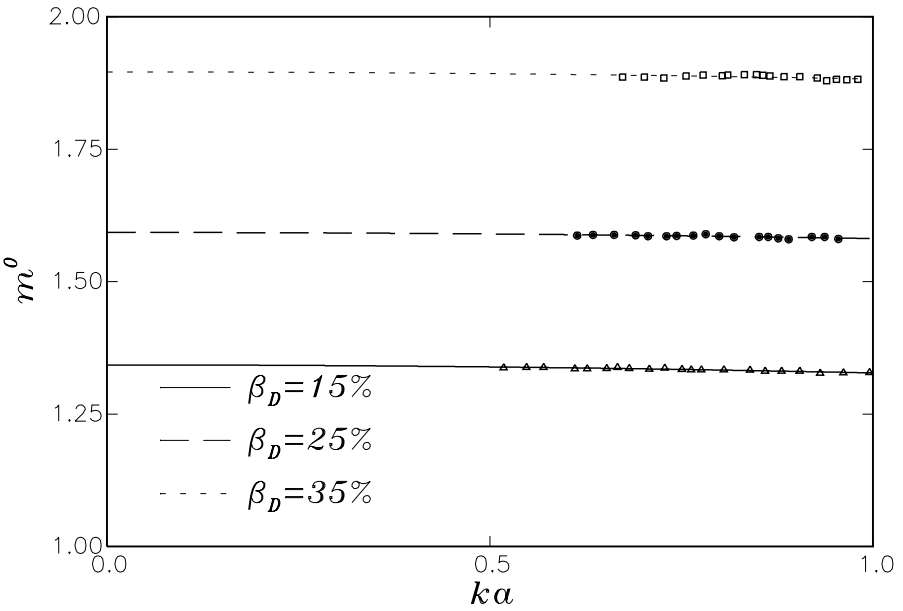

Fig. 13. The quantity m^0 appearing in the expression of the hydrodynamic couple acting on spinning particles in Eq. (6.8) as a function of ka for $\beta_{\mathrm{D}}^0 = 15\%$ (triangles), 25% (black circles) and 35% (squares); the lines are least-squares fits of the form $A + B(ak)^2$.

Upon comparing (6.1) with (6.5) we deduce that

$$\frac{\mu_{\mathrm{eff}} - \mu_{\Delta}}{\mu_{\mathrm{C}}} U^c = s_S^{\Omega}; \tag{6.9}$$

from (6.6) and (6.2)

$$V_1 U^c = v^c - k^2 a^2 (V_3 - (1/2)V_4 - V_9) U^c, \tag{6.10}$$

from (6.3) and (6.7)

$$A^c = -F_1 U^c - a^2 k^2 (F_3 - (1/2)F_4 - F_9) U^c, \tag{6.11}$$

and from (6.4) and (6.8)

$$m^0 = L_1, \tag{6.12}$$

$$m^s = [(1/2)L_1 - L_4 + k^2 a^2 (L_3 - (1/2)L_9)] U^c. \tag{6.13}$$

In the limit $ak \to 0$,

$$V_1 = \lim_{ak \to 0} \frac{v^c}{U^c}, \quad F_1 = -\lim_{ak \to 0} \frac{A^c}{U^c}, \quad L_1 = \lim_{ak \to 0} m^0. \tag{6.14}$$

The parameter L_1 had not been determined in the porous medium case, while the other two were. Upon comparing the results given by (6.9) and (6.14) with those found earlier, we can test the independence of the proposed closure on the particular flow simulation. This comparison will be made in the following section.

7. Discussion

In papers I and II, the present systematic method for the derivation of closure relations was applied to the three cases of particles subject to the same force, the same torque and a simple shear. In the present paper, we have applied the technique to particles moving with the same translational or angular velocity. If true constitutive equations exist, the closure relations and the coefficients appearing in them should be the same for all these cases.

Consider the gravitational settling of a uniform suspension. In this case, all gradients vanish except ∇p_m and all particles are subjected to the same force $\mathbf{b} = \rho_D v \mathbf{g}$, where ρ_D is the particle density and $\mathbf{g}$ the gravity force per unit mass; upon eliminating ∇p_m between (2.3) and (2.6) we thus find $\mathbf{f} = \mathbf{b}$ or, from the closure relation (2.15) with $F_1(\beta_D)$ expressed in terms of the hindered settling function $\Phi(\beta_D)$ calculated in papers I and II,

$$\mathbf{f}_{\text{sedim}} = -\frac{9\beta_C}{2\Phi(\beta_D)}\frac{\mu_C}{a^2}\mathbf{u}_m. \tag{7.1}$$

This situation may be contrasted with the pressure-driven flow through a uniform porous medium considered in the present paper. The continuous-phase momentum equation (2.3) gives

$$\beta_C \nabla p_m = \beta_D \mathbf{f}_{\text{porous}}, \tag{7.2}$$

or, since in the uniform case, from (3.10) and (4.13), $\nabla p_m = \nabla p_\infty$ and $\mathbf{u}_m = \mathbf{U}_0$, from (4.5) and (4.6),

$$\mathbf{f}_{\text{porous}} = -\frac{9\beta_C}{2K(\beta_D)}\frac{\mu_C}{a^2}\mathbf{u}_m. \tag{7.3}$$

For the two expressions for the interphase force to be equal, it would evidently be necessary that the hindered settling function Φ equal the dimensionless permeability K, which is not supported by the numerical evidence as shown in Table 3.

At a fundamental level, this discrepancy is not surprising as, for a prescribed equal force on the particles (as, e.g., in sedimentation), the microscopic particle velocities must be found from

$$\mathbf{F} = \mathscr{R}\mathbf{W}, \tag{7.4}$$

Table 3
Comparison among the values of the closure coefficients K, V_1, and Ψ as derived from the sedimentation and applied couple simulations of paper II, and the porous medium and spinning particles simulations of the present paper

β_D (%)	K			V_1			Ψ	
	Sedim.	Por. md.	Spinn.	Sedim.	Por. md.	Spinn.	Couple	Spinn.
15	0.352	0.263	0.243	0.0531	0.0690	0.0623	0.789	0.671
25	0.188	0.140	0.133	0.145	0.186	0.166	0.670	0.943
35	0.0989	0.0726	0.0784	0.315	0.414	0.351	0.557	1.11

where $\mathscr{R}$ is the resistance matrix and the vectors $\mathbf{F}$, $\mathbf{W}$ contain the forces and velocities of all the particles. However, if an equal velocity is prescribed for the particles (as in the case of a porous medium), the force acting on them must be found from

$$\mathbf{W} = \mathscr{M}\mathbf{F}, \tag{7.5}$$

where $\mathscr{M}$ is the mobility matrix. From these equations, after taking the ensemble average, we have

$$\overline{\mathscr{R}^{-1}}\mathbf{F} = \overline{\mathbf{W}}, \quad \text{and} \quad \overline{\mathscr{M}^{-1}}\mathbf{W} = \overline{\mathbf{F}}, \tag{7.6}$$

respectively, given that in the first case the forces are the same for all the particles while in the second case the velocities are equal. For these two relations to be compatible it would evidently be necessary that

$$(\overline{\mathscr{R}^{-1}})^{-1} = \overline{\mathscr{M}^{-1}}, \tag{7.7}$$

which, while valid before averaging, is not necessarily true after taking the ensemble average.

A parallel argument can be made for the case of particle rotation. In paper II, it was shown that L_1 was related to the hindrance function for rotation $\Psi(\beta_D)$ (also called dimensionless vortex viscosity, see Brenner, 1984) by

$$\Psi = \frac{6\beta_D}{L_1}. \tag{7.8}$$

In paper II, Ψ was calculated from simulations in which the particles were subjected to equal couples; those values are shown in Table 3, where they are compared with those found using the L_1 of the previous section. The two sets of results are clearly quite different and even exhibit an opposite trend with increasing β_D. This qualitative difference arises from the slower growth of L_1 with β_D in the spinning particle case.

While this argument justifies the fact that the two expressions (7.1) and (7.3) for the interphase force and the corresponding ones for the couple are not consistent, it does lead to the somewhat perplexing conclusion that an averaged description as the one attempted here and in many other studies appears to be insufficient to completely characterize the system.

Superficially, the situation is similar to results of Almog and Brenner (1997, 1998), who compared the motion of a sphere in a suspension for a prescribed force and a prescribed velocity finding that the effective viscosity of the suspension differs in the two cases; a similar comparison for the rotational motion with a given couple or a given angular velocity also revealed differences (Almog and Brenner, 1998). The root of the differences found in these studies is in the way the flow determines the spatial probability distribution of the suspended spheres, but this explanation does not apply in our case as the same set of configurations was used in all the flow situations considered in this and in the earlier papers.

It would then appear that, if a satisfactory closure exists at all, it must contain one or more additional variables which must differ for the two cases of equal forces and equal velocities and, even if such a description is possible, the problem remains of finding evolution equations for these additional parameters. Furthermore, the results of Almog and Brenner (1997, 1998) suggest that the spatial particle probability distribution, as affected by different flow situations, would also play a role.

It might be tempting to argue, as one of the reviewers of this paper did, that "a porous medium and a suspension are two quite different media, and there is no reason to expect that they should be governed by the same equations, let alone the same coefficients." At one level, this is certainly true and, as a matter of fact, several authors have commented on the difference between the two situations starting with Brinkman (1947), (see also e.g., Lundgren, 1972; Saffman, 1973). But this position evades the issue: in the reference frame in which the mean particle velocity vanishes, a sedimenting suspension and a porous medium are indistinguishable if described solely in terms of velocities, volume fraction, and mean pressure (augmented, in the former situation, by the gravitational potential). Furthermore, one may conceptually imagine a continuous transition from one case to the other by allowing the particles to be attached less and less loosely to certain fixed sites. How is this information to be incorporated into the averaged equations?

A possible additional variable to introduce in the theory is the standard deviation of the particle velocity σ_w (and perhaps the corresponding quantity for the angular velocity), which might be related to some form of "granular temperature" (see e.g., Jenkins and Louge, 1997; Koch and Sangani, 1999). Such a variable would be compatible with linearity and would vanish in the porous medium case but not for sedimentation. In principle, this hypothesis can be tested by the same techniques used in this work: consider a sedimentation case in which the settling particles have different masses assigned according to a certain probability distribution and calculate the resulting velocity probability distribution. Then carry out a "porous medium" simulation by assigning the particle velocities according to the probability distribution determined from the sedimentation simulation. If the hypothesis is correct, the closure coefficients found in the two cases should agree. One may also follow the opposite route starting with prescribed unequal velocities, calculating the force probability distribution, etc.

The presence of additional – or "hidden" – variables might also justify the perplexing fact encountered in our work that, while the averaging of some quantities converges relatively fast and gives rise to smooth dependencies on ak, for other quantities convergence of the average is more problematic (see for example Figs. 10, 11 and 16 in paper I or Fig. 2 in paper II).

Looking back to the simulations of papers I and II with the hindsight of the possible existence of hidden variables, one must conclude that quantities such as σ_w would not be equal in the three situations simulated in those papers. Nevertheless, the effective viscosity was found to agree in the three cases, which shows this concept to be robust and apparently independent of the flow considered (other than, of course, a possible indirect effect through the dependence of the particle probability distribution function). Two other closure parameters that could in principle be obtained from more than one type of flow situation were the two additional viscosities μ_Δ and μ_∇ the determination of which, however, as explained in detail in paper II, was uncertain. Upon comparing those values with the present ones (Table 4) again we find inconsistencies. Thus, while our numerical simulations strongly imply that the corresponding terms are necessary to parameterize the simulation results (in the sense that, were they omitted, certain quantities should vanish in clear conflict with the numerical evidence), all we can say at this point is that we have been unsuccessful in determining the values of these parameters.

Finally, in paper II, Q_2 was found by combining results for the two cases of sedimentation and imposed shear. The corresponding results, as shown in Table 4, are at variance with the present

Table 4
Comparison between the values of the closure coefficients $\mu_{\text{eff}} - \mu_{\Delta}$, $\mu_{\nabla}/\mu_{\text{C}}$, and Q_2 derived in paper II and the porous medium simulations of the present paper

β_{D} (%)	$(\mu_{\text{eff}} - \mu_{\Delta})/\mu_{\text{C}}$			$\mu_{\nabla}/\mu_{\text{C}}$		Q_2	
	Sedim.	Por. md.	Spinn.	Paper II	Por. md.	Paper II	Por. md.
15	0.112	0.150	0.410	1.17	0.392	1.15	~ 0
25	0.153	0.174	0.224	2.65	0.989	2.39	1.03
35	$\sim$0	0.0391	0.197	7.39	3.06	5.55	4.70

ones determined for the porous medium. This finding suggests the possibility that the ''true'' values of Q_2 could be different for the two situations of paper II so that combining them might have been incorrect.

8. Conclusions

The great effort devoted over the past several decades to the formulation of averaged equations for multiphase flow is based on the tacitly accepted postulate that such a description is possible independently – at least over a practically useful range – of the particular flow situation. In particular, in the widely used class of so-called 'two-fluid models', it is assumed that an average description solely phrased in terms of the average velocities, volume fraction, and mixture pressure is possible. Our results furnish the first conclusive test of this widely held assumption for the particular case of particles suspended in Stokes flow – and they suggest that it is false for the general case of spatially non-uniform flows.

The implications of these findings are unclear at present. It may be that a useful averaged description can be found with the simple addition of one or a few additional variables, as discussed in the previous section, or that only specialized models for different classes of flows can be formulated, which cannot be reconciled with each other. This is obviously an important question that can only be answered by further work; the techniques developed in the present series of papers can be adapted to this task.

As a final point, we would like to note that, when the closure relations (2.11)–(2.15) are substituted into the momentum equation (2.3), the term multiplying $\nabla^2\mathbf{u}_{\text{m}}$, to which one can refer as the *Brinkman viscosity* μ_{B}, is

$$\frac{\mu_{\text{B}}}{\mu_{\text{C}}} = \frac{\mu_{\text{eff}} - \mu_{\Delta}}{\mu_{\text{C}}} + \frac{1}{2}R_1 + R_4 + V_1 + 6\pi a^2\beta_{\text{C}}\left(F_3 - \frac{1}{2}F_4 - F_9\right). \tag{8.1}$$

It seems highly probable that this expression cannot be reduced to any simple combination of μ_{eff} and μ_{C}, which explains the failure of past attempts along these lines. Unfortunately, since we have not been able to calculate all the coefficients appearing in this relation, we cannot test this conclusion against the direct determinations of μ_{B} in the literature (see e.g., Martys et al., 1994).

Acknowledgements

The authors express their gratitude to Dr. Michael Tanksley for his help in the early stages of this work and to the Engineering Research Program of the Office of Basic Energy Sciences at the Department of Energy for support under grant DE-FG02-99ER14966.

Appendix A. The dilute limit

When adapted to the present case, the momentum equation derived for the continuous phase in Zhang and Prosperetti (1997) for the dilute limit is (see also the Appendix to paper I)

$$0 = -\frac{1}{\mu_C}\nabla p_m + \beta_D \mathbf{f} + \nabla\cdot\left[2\left(1+\frac{5}{2}\beta_D\right)\mathbf{E}_m\right] + \frac{3}{4}\nabla^2(\beta_D \mathbf{u}_A) + 3\nabla\times(\beta_D\omega). \tag{A.1}$$

The expression given in the same paper for the mean hydrodynamic force reduces here to

$$\beta_D v\mathbf{f} = -6\pi\mu_C a\beta_D\left(\mathbf{u}_m + \frac{a^2}{6}\nabla^2\mathbf{u}_m\right). \tag{A.2}$$

For the two situations studied in this paper, the solution of these equations is readily found; we can carry both together if we write

$$\beta_D = \beta_D^0 + \beta_D^s\epsilon_s, \tag{A.3}$$

$$\frac{1}{\mu_C}p_m = -\frac{9}{2a^2}P^0\mathbf{U}^0\cdot\mathbf{x} + \frac{9}{2ka^2}P^c\epsilon_c\mathbf{U}^0\cdot\mathbf{m}, \tag{A.4}$$

$$\mathbf{u}_m = \mathbf{U}^0 + U^s\epsilon_s\mathbf{U}_\perp^0 + U^c\epsilon_c\boldsymbol{\Omega}_\perp. \tag{A.5}$$

When these expressions are substituted into Eqs. (A.1) and (A.2), one finds the following expressions for the coefficients arising in the parameterizations presented in Section 4:

Porous medium ($\boldsymbol{\Omega}_\perp = 0$):

$$P^0 = \beta_D^0, \quad P^c = \left(1-\frac{a^2k^2}{6}\right)\beta_D^s, \qquad U^s = -\left(1-\frac{a^2k^2}{6}\right)\frac{\beta_D^s}{\beta_D^0}. \tag{A.6}$$

Imposed angular velocity ($\mathbf{U}^0 = 0$):

$$U^c = \frac{2}{3}ka\frac{\beta_D^s}{\beta_D^0}. \tag{A.7}$$

All other quantities not explicitly given are equal to zero. The quadratic dependence of β_D^s on ak shown in (3.7) justifies the k-dependence assumed in writing the coefficients of Section 4.

References

Almog, Y., Brenner, H., 1997. Non-continuum anomalies in the apparent viscosity experience by a test sphere moving through an otherwise quiescent suspension. Phys Fluids 9, 6–22.

Almog, Y., Brenner, H., 1998. Apparent slip at the surface of a small rotating sphere in a dilute quiescent suspension. Phys Fluids 10, 750–752.

Brenner, H., 1984. Antisymmetric stress induced by the rigid-body rotation of dipolar suspensions. Int. J. Eng. Sci. 22, 645–682.

Brinkman, H.C., 1947. A calculation of the viscous force exerted by a flowing fluid on a dense swarm of particles. Appl. Sci. Res. A1, 27.

Jenkins, J.T., Louge, M.Y., 1997. On the flux of fluctuation energy in a collisional grain flow at a flat, frictional wall. Phys. Fluids 9, 2485–2490.

Koch, D.L., Sangani, A.S., 1999. Particle pressure and marginal stability limits for a homogeneous monodisperse gas-fluidized bed: kinetic theory and numerical simulations. J. Fluid Mech. 400, 229–263.

Lundgren, T.S., 1972. Slow flow through stationary random beds and suspensions of spheres. J. Fluid Mech. 51, 273–299.

Marchioro, M., Prosperetti, A., 1999. Conduction in non-uniform composites. Proc. R. Soc. London A 455, 1483–1508.

Marchioro, M., Tanksley, M., Prosperetti, A., 1999. Mixture pressure and stress in disperse two-phase flow. Int. J. Multiphase Flow 25, 1395–1429.

Marchioro, M., Tanksley, M., Prosperetti, A., 2000. Flow of spatially non-uniform suspensions. Part I: Phenomenology. Int. J. Multiphase Flow 26, 783–831.

Marchioro, M., Tanksley, M., Wang, W., Prosperetti, A., 2001. Flow of spatially non-uniform suspensions. Part II: Systematic derivation of closure relations. Int. J. Multiphase Flow 27, 237–276.

Martys, N., Bentz, D.P., Garboczi, E.J., 1994. Computer simulation study of the effective viscosity in Brinkman's equation. Phys. Fluids 6, 1434–1439.

Mo, G., Sangani, A.S., 1994. A method for computing Stokes flow interactions among spherical objects and its application to suspensions of drops and porous particles. Phys. Fluids 6, 1637–1652.

Saffman, P.G., 1973. On the settling speed of free and fixed suspensions. Stud. Appl. Math. 52, 115–127.

Zhang, D.Z., Prosperetti, A., 1997. Momentum and energy equations for disperse two-phase flows and their closure for dilute suspensions. Int. J. Multiphase Flow 23, 425–453.